Proceedings of the 6th International Conference on Gas Hydrates (ICGH 2008),
Vancouver, British Columbia, CANADA, July 6-10, 2008.

A STUDY OF HYDRATE FORMATION AND DISSOCIATION FROM HIGH WATER CUT EMULSIONS AND THE IMPACT ON EMULSION INVERSION

David P. Greaves, John A. Boxall, James Mulligan, E. Dendy Sloan, and Carolyn A. Koh*
Center for Hydrate Research
Department of Chemical Engineering
Colorado School of Mines
1600 Illinois St, Golden, CO
USA

ABSTRACT

Methane hydrate formation and dissociation studies from high water content (>60 vol% water) – crude oil emulsions were performed. The hydrate and emulsion system was characterized using two particle size analyzers and conductivity measurements. It was observed that hydrate formation and dissociation from water-in-oil (W/O) emulsions destabilized the emulsion, with the final emulsion formulation favoring a water continuous state following re-emulsification. Hence, following dissociation, the W/O emulsion formed a multiple o/W/O emulsion (60 vol% water) or inverted at even higher water cuts, forming an oil-in-water (O/W) emulsion (68 vol% water). In contrast, hydrate formation and dissociation from O/W emulsions (≥71 vol% water) stabilized the O/W emulsion.

Keywords: Agglomeration, hydrate dissociation, emulsion, emulsion inversion, FBRM, PVM

INTRODUCTION

Clathrate hydrate formation presents a serious challenge to the petroleum industry. The low temperature and high pressure conditions necessary for hydrate formation between natural gas and water are frequently satisfied in petroleum pipelines. Upon formation, hydrate accumulation and agglomeration ultimately forms a plug, blocking the flow through the pipeline. These plugs can be costly and dangerous to remove and can lead to a significant loss in production [1,2].

A variety of inhibitors are utilized by the petroleum industry to prevent hydrate plug formation; however, these inhibitors are not designed for high water content production. Thermodynamic inhibitors, which shift the pressure-temperature hydrate equilibrium curve, and kinetic inhibitors, which delay hydrate formation, are injected proportional to the water volume (or cut), meaning that at higher water cuts, more and more inhibitor is necessary. Alternatively, anti-agglomerants, which allow for hydrates to form but prevent hydrate particle agglomeration, are typically not designed to operate at water cuts above 60 vol.% [2].

As oil and gas are produced from less profitable and/or older wells, there is an increased likelihood of higher water cuts, resulting in more costly inhibition strategies. Various authors have studied hydrate formation from low water cut emulsions with few studies approaching 60 vol% or more [3,4,5,6]. The purpose of this work is to increase the understanding of hydrate formation and dissociation from these high water content (> 60 vol%) emulsions of water-in-oil (W/O) and oil-in-water (O/W).

* Corresponding author: Phone: +1 303 273 3237 Fax: +1 303 273 3730 E-mail: ckoh@mines.edu

For W/O emulsions, it has been proposed that hydrate initially forms as shells around water drops [6,7]. In this model, shells form rapidly first, followed by slow conversion of the internal, trapped water to hydrate, which is limited by mass transfer of the hydrate guest molecule through the shell.

Hoiland et al. [8,9] have considered the interaction of hydrates and emulsions at high water cuts as they explored how the presence of hydrate particles can promote or delay the inversion of a water-crude oil emulsion (emulsion inversion describes the change in emulsion type from O/W to W/O or vice-versa as discussed below). Hoiland et al. formed Freon hydrates *in situ* from different water-in-crude oil emulsions at low water cut (enough water to stoichiometrically consume all of the Freon in hydrate formation). Water was then added incrementally until the emulsion inverted from W/O to O/W.

By comparing the water cut at inversion with hydrates to that without hydrates, Hoiland et al. [8,9] predicted the relative wettability of the hydrate particles (See Binks [10] for relationship between inversion and wettability). The results showed good correlation between the crude oil's plugging behavior tested in a flowloop and the experimental wettability; crude oils which formed oil-wet hydrates (through adsorption of natural components) showed no signs of plugging in the flow loop.

The goals of this work differ from that of Hoiland et al. [8,9]. This work investigates how hydrate formation and dissociation can cause an existing emulsion to destabilize and potentially invert, as opposed to increasing the water cut to cause inversion. Furthermore, the major goal of this work was to develop a conceptual picture for hydrate formation and dissociation from various high water cut scenarios (W/O, O/W, etc.).

As part of this work, the impact of hydrate formation and dissociation on the emulsion type and inversion was studied. Inversions are generally classified into two categories: transitional and catastrophic [11,12]. Transitional inversions are typically associated with gradual change, including the formation of a microemulsion. Such inversions occur when the system properties are adjusted, including salinity, surfactant type, temperature, etc. Catastrophic inversions occur much more rapidly, commonly by increasing the dispersed phase content (e.g. the inversion experiments of Hoiland et al.). Multiple emulsions such as o/W/O (oil droplets within water drops dispersed in oil) or similarly w/O/W may form near the catastrophic inversion [13].

The type of emulsion is generally determined by the relative amounts of water and oil (the water-oil-ratio or WOR), the surfactant concentration, and the formulation. The WOR controls the emulsion type at the extremes – water continuous with high water cuts and oil continuous at low water cuts. The formulation describes the thermodynamically preferred emulsion state (either water or oil continuous) and can be a single variable (like temperature) or a more complex variable accounting for the surfactant behavior at the interface. Increasing the formulation can lead to a transitional inversion from O/W to W/O and vice-versa for decreasing the formulation [11,12,14,15].

EXPERIMENTAL METHODS

Experiments were performed in a high pressure reaction autoclave cell with methane gas (ultra high purity grade from Matheson Tri-Gas®) as the hydrate former. A schematic of this reaction vessel is shown in Figure 1. The autoclave cell total volume was 1.89 liters, which included the placement of a solid metal false bottom (labeled i), and was pressure rated to 104 bar. Two particle size analyzers (PSA), the Particle Video Microscope (PVM) and the Focused Beam Reflectance Measurement (FBRM), were inserted into the autoclave cell 180° from each other and at 45° angles to the vertical, labeled a and b, respectively. Tri-clamp fittings ensured the pressure seals at the PSA probe insertion points.

The FBRM probe consists of a laser which scans the fluid immediately in front of the probe window. The laser reflects back when scanning a particle or droplet. The FBRM can measure particle chords between 1-1000 μm. The product of the scan speed (4 m/s) and the scanning time for an object represents a chord length. Measured chord lengths are then grouped or binned into different chord length sizes to generate a chord length distribution (CLD). Statistics such as size and chord count can also be measured to monitor changes in the system.

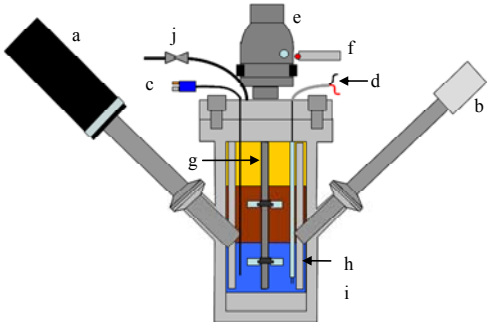

Figure 1. Autoclave cell schematic with attached probes and sensors: (a) PVM probe; (b) FBRM probe; (c) thermocouple; (d) conductivity meter; (e) MagneDrive; (f) tachometer; (g) impeller system; (h) baffles; (i) false bottom; (j) gas inlet.

The PVM probe consists of a digital camera, which provides *in situ* images of the particles or droplets with a field of view of 826 µm x 619 µm and clear resolution in this work for objects larger than 20 µm. Six lasers illuminate the area in front of the probe window for imaging. For more detailed information on these two probes, the reader is referred to the FBRM and PVM user manuals [16,17].

To prevent hydrate deposition on the probe windows, the probes were cleaned in a sequence of rinses with toluene, acetone, and hydrogen peroxide. Finally, the probe windows were immersed in a 20% dichlorodimethylsilane-80% toluene solution to create a more hydrophobic surface and, thereby, limit the adhesion of water and hydrate to the probe window surface [18].

Mixing was provided by two six-blade turbine impellers (labeled g on Figure 1) located 5.1 and 12.7 cm from the top of the false bottom (the total internal cell dimensions being 22.9 cm in height and 10.2 cm in diameter). The impellers and shaft were connected inline to a MagneDrive II magnetically coupled stirrer (Autoclave Engineers®) and mounted to the top of the cell. The MagneDrive II (labeled e) was belt driven by an external motor (not shown). Using this motor, the shaft and impellers could be rotated at speeds up to 600 rpm safely, as measured by a tachometer (labeled f). Constant volume experiments were performed in the autoclave cell, meaning that as hydrate formed the cell pressure dropped as gas is concentrated in the hydrate. A data acquisition system (DAQ) measured the temperature and pressure from the thermocouple (labeled c) and the pressure transducer on the inlet gas line (labeled j), respectively, during the hydrate event.

A custom-made conductivity meter (labeled d) was constructed to withstand high pressures and monitor the continuous phase of the emulsion. A Conax-Buffalo® electric feedthrough was mounted to the top of the autoclave cell with two wire leads on either end. The internal lead wires were insulated and ran to the bottom of the cell, with the copper wire exposed 1.6 cm at the end of each wire. The two wire tips (with aluminum solder added for improved strength) were approximately 0.32 cm apart and were located near one of the four baffles, 2.5 cm from the top of the false bottom insert. The external side wires were attached in circuit to the DAQ and a nine volt battery, which provided the voltage for the circuit.

The DAQ recorded the voltage in the circuit, which could be used intuitively to identify the external phase. Low voltage, typically less than one volt, confirmed that the oil was the continuous phase, with the emulsion most likely being either W/O or o/W/O, as oil has a high electrical resistance. Higher voltage (closer to nine volts) implied a water continuous phase. Salt (3.5 wt% NaCl) was added to the water phase before forming the emulsion to increase the conductivity of the emulsion. Conductivity measurements in this paper are relative as they are in volts, and do not account for properties such as the surface area and distance between electrodes. For more details on the apparatus and probes see Greaves [19].

The desired volume of salt water was added to the autoclave cell followed by the desired volume of crude oil (1180 ml total liquid, salt-free basis). Conroe crude oil was used for all of these experiments; this oil has a relatively low viscosity for crude oils (between 5 and 10 cP at 5˚C over an approximate range of shear rates from 3-300 s^{-1}) and is relatively transparent, making it ideal for observation with the PVM. The interfacial tension of Conroe crude in water was found to be 24.6 mN/m with pure water at 4˚C [6]. It is important to note that crude oil, including Conroe crude oil, typically contains some natural emulsifiers which stabilize W/O emulsions; therefore, it was not necessary to add surfactant to the system [15,20].

With the liquid loaded in the cell, a Teflon ring was placed on the top of the cell for sealing. The lid assembly (with MagneDrive) was then lowered onto the cell and securely bolted. The autoclave cell was then placed in a cooling bath initially at 20°C, and the mixer was turned on, emulsifying the water-oil system at 400 rpm.

The cell was then pressurized with methane gas to 76.8 bar. After a steady size distribution of water drops in oil or vice-versa had been reached as measured by the FBRM, the cell was cooled to 4°C. Hydrate ultimately formed at this temperature, causing the pressure to drop and the system temperature to rise as hydrate formation is an exothermic process. Hydrate was allowed to form for at least four hours before heating the emulsion to 20°C to dissociate the hydrate, where upon the pressure returned to 76.8 bar.

EXPERIMENTAL RESULTS

Methane hydrate was formed in the autoclave cell from water-Conroe oil emulsions at water cuts of 60, 68, 71, 75, and 100 vol% water. Without hydrate present, emulsification experiments between 60-68 vol% water resulted in an oil continuous emulsion, and experiments between 71-100 vol% water resulted in a water continuous emulsion. Therefore, the catastrophic emulsion inversion for this system, without hydrates, was isolated to the range of 68-71 vol%. The following results are categorized according to the emulsified state prior to formation, either oil or water continuous.

Hydrate formation from W/O emulsions

The observed hydrate formation and dissociation from W/O emulsions at high water cuts followed the conceptual pictures shown in Figure 2. Due to the excess water in the system, when hydrate formed from the W/O emulsion, it rapidly agglomerated as shown in Figure 2b. Dissociation of these large agglomerates led to the formation of large water drops (relative to the original drops) in the system in Figure 2c. A free water phase may also have formed at this time. During dissociation and re-emulsification of these large water drops, one of two paths was observed – the emulsion either ended as an oil continuous W/O (Figure 2e) emulsion (usually o/W/O) or at even higher water cuts (closer to the inversion), inverted to an O/W (Figure 2d) or w/O/W emulsion. Details are provided in the following sections for the 60 and 68 vol% water in Conroe oil experiments, representing the non-inverting and the inverting W/O systems, respectively.

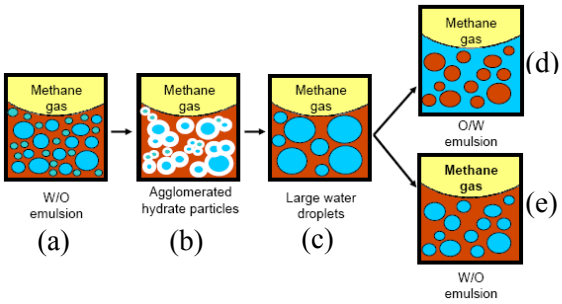

Figure 2. Hydrate formation from a W/O emulsion pressurized with a hydrate forming gas: (a) initial emulsion; (b) agglomerated hydrate particles; (c) dissociated droplets; (d) final inverted O/W emulsion; (e) or final W/O emulsion. (d) or (e) depends on fluid properties, shear history, water cut, temperature, etc. The liquid-gas interface is curved to represent the autoclave cell mixing behavior.

Oil continuous emulsions (60 vol%)

Emulsifying 60 vol% salt water with Conroe oil (on a salt free basis) formed a W/O emulsion as measured by the low relative conductivity (≈0.35 V) in the system. The relatively dense packing of droplets seen in the PVM images also suggested that water was the dispersed phase; dense packing implies that the phase with a higher volume is dispersed.

The image sequence in Figure 3 shows the initial emulsion, the emulsion with hydrates, and the emulsion during and after dissociation. Figure 4 is the matching conductivity and temperature response for the entire experiment. In Figure 4, at nucleation, the temperature rose 1.5°C (due to exothermic hydrate formation) and was matched by a dramatic drop in pressure (not shown). Nucleation and dissociation are marked by the two vertical lines in Figure 4 (and Figures 7 and 11).

The conductivity simultaneously increased with nucleation in Figure 4 and remained high until dissociation was complete. In fact, as dissociation started, the conductivity temporarily increased before developing significant scatter.

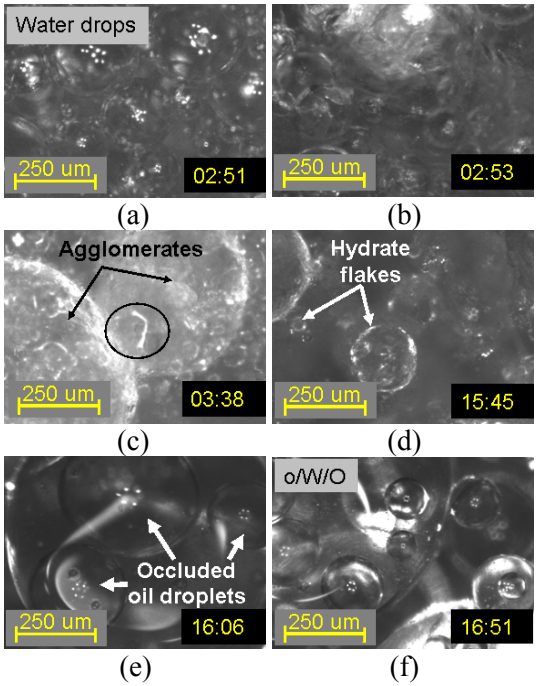

Figure 3. 60 vol% water dispersed in Conroe oil: (a) initial emulsion (W/O); (b) initial hydrate formation one min. after nucleation; (c) large hydrate agglomerates and thin hydrate film (circled); (d) hydrate flakes on water droplets 15 min. after the start of dissociation; (e) initial formation of an o/W/O emulsion; (f) final o/W/O emulsion.

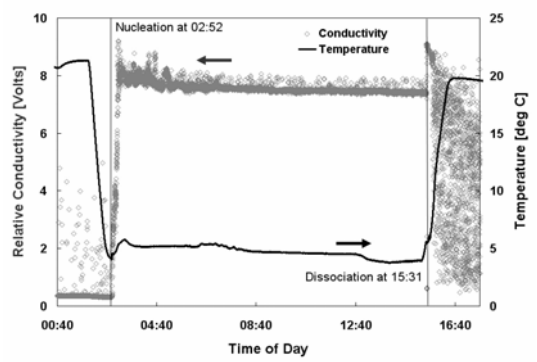

Figure 4. Conductivity and temperature measurements of hydrate formation and dissociation for 60 vol% water in Conroe oil.

The PVM images provide a physical explanation for the conductivity results. With hydrate formation the morphology of the droplets changed immediately, and rapid hydrate agglomeration was visible as shown in Figure 3b. High water cut facilitates agglomeration as water wets the hydrate particles, effectively increasing the particle adhesion [21,22]. With continued hydrate formation from W/O emulsions, a hydrate film typically formed on the PVM window, despite the coating. However, the film was thinner with than without the coating. Large agglomerates (>500 μm) could still be seen in the PVM such as those in Figure 3c beyond the thin film on the window.

It is believed that the conductivity increased with hydrate nucleation because wet hydrate particles and agglomerates stuck to the conductivity electrodes. This phenomenon is demonstrated in Figure 5. The adhesion of wet hydrates to the electrodes provided a higher conducting bridge (2) than the W/O emulsion existing prior to nucleation (1). With the start of dissociation, excess surface water would have formed on the hydrate between the electrodes, providing an even more conductive path and hence a higher voltage (3). With additional heating, the hydrate dissociated enough that the agglomerate (which provides the physical bridge for the liquid) was swept away from the electrodes, causing the conductivity to fall (4).

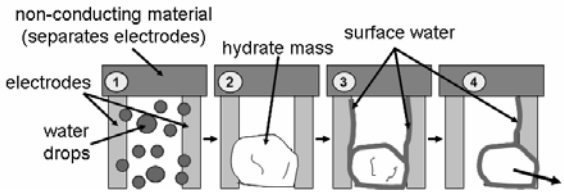

Figure 5. Proposed sequence for dissociation of agglomerate affixed to the conductivity electrodes: (1) water droplets in oil; (2) hydrate agglomerate sticks to electrodes; (3) dissociation begins - liquid bridge forms between electrodes; (4) further dissociation causes agglomerate to shrink and be swept away.

As shown in Figure 3d, as dissociation began, hydrate flakes were visible which gathered at the water-oil interface. With continued dissociation, the flakes completely dissociated while simultaneously an o/W/O multiple emulsion formed (Figures 3e and 3f). The conductivity was necessary to identify the continuous phase for both simple and complex emulsions. The low conductivity on average following dissociation implies that the continuous phase was oil; hence, the multiple emulsion seen in the PVM images must be o/W/O. The occlusion of the oil droplets in the water drops led to large swollen water drops which could be approaching the same size scale as the electrode separation. The voltage readings in Figure 4 fluctuated with significant noise following dissociation as the conductivity meter measured both the continuous oil phase (low

conductivity) and the passing of swollen water drops (high conductivity).

Oil continuous, near inversion (68 vol%)

When the water cut was increased to 68 vol%, the emulsion also began as a W/O emulsion but inverted to an O/W and ultimately a w/O/W emulsion as shown in the images in Figure 6 following dissociation. The conductivity (See Figure 7) of the initial emulsion was again low prior to nucleation, confirming that droplets seen in Figure 6a were water drops dispersed in oil. Upon nucleation, identified by the exothermic temperature rise, there was a sudden increase in the conductivity similar to the conductivity response in Figure 4, most likely from hydrate adhesion to the electrodes. With the start of dissociation, there was no sharp rise in conductivity as there was for the 60 vol% water case. Instead, the average voltage after dissociation was higher (6.6 volts in Figure 7) and remained high, though it again fluctuated with noise.

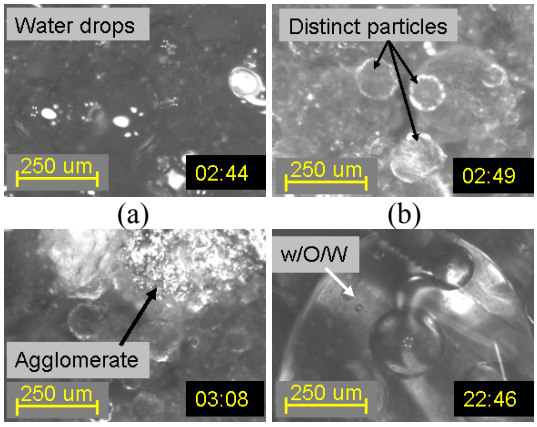

Figure 6. 68 vol% water in Conroe oil: (a) initial emulsion (W/O); (b) hydrate formation 4 min. after nucleation; (c) large agglomerates; (d) w/O/W emulsion 69 min. after start of dissociation.

The high average voltage following dissociation suggests that the emulsion completely inverted to be water continuous. PVM images like that in Figure 6d show that the emulsion eventually ended as a multiple emulsion; high conductivity implies that the multiple emulsion was w/O/W. The increased noise in conductivity is due to the large swollen oil drops in the multiple emulsion discussed later.

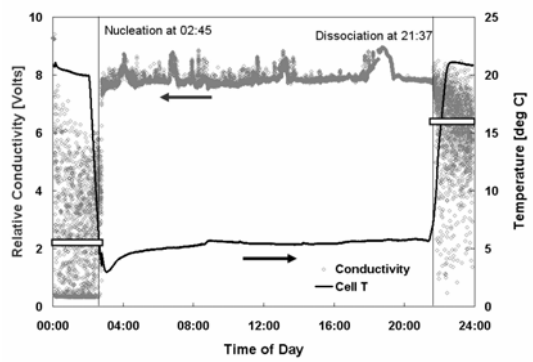

Figure 7. Conductivity and temperature measurements for hydrate formation and dissociation from 68 vol% water in Conroe oil. The bold rectangles are the average conductivity values before and after the hydrate event.

Figures 6b and 6c are shown to demonstrate that for hydrate formation from W/O emulsions, large agglomerates as well as distinct hydrate particles are visible in the system. These images are similar to images for all the formation experiments for oil continuous emulsions (including 60 and 68 vol%). The same types of hydrate (agglomerates and particles) are also observed for the water continuous systems.

The FBRM chord length distributions and statistics can also be used to identify the emulsion changes. As discussed in Greaves [19], without the conductivity measurements and PVM images, it is difficult to know the emulsion type from the FBRM results. The FBRM cumulative distributions identify a clear growth in chord length size from before hydrate nucleation to after dissociation for the 68 vol% experiment as shown in Figure 8. Upon dissociation the average chord length increases from 22 to 42 µm, and the entire distribution shifts to the right as the FBRM measures larger droplets, resulting in larger overall measured chord lengths.

Images from the PVM provide the physical meaning for the change in the FBRM results from before to after the hydrate event. Following dissociation, a multiple w/O/W emulsion formed as previously discussed. The occlusion of water droplets caused the oil drops dispersed in water to swell forming larger drops. The measurement of these swollen oil drops in the w/O/W emulsion compared with the initially emulsified water drops in the W/O emulsion (pre-nucleation) accounts for the growth in large chord measurements.

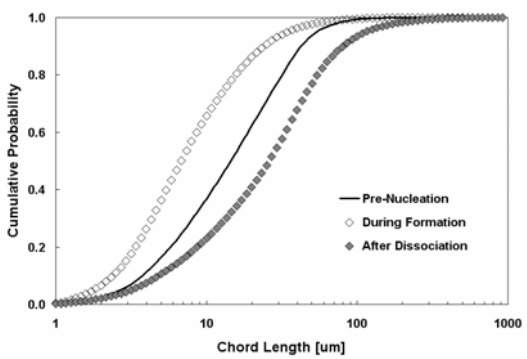

Figure 8. FBRM cumulative CLDs for 68 vol% water in Conroe oil. Distributions represent the average of 10 FBRM measurements. Pre-nucleation results are from 10 min. prior to nucleation (at 4°C), during formation results are taken at the peak in measured counts 2 hr. after nucleation, and after dissociation is taken 3 hr. after the start of dissociation (at 20°C).

The FBRM cumulative distribution with hydrates presented in Figure 8 is reported to demonstrate the challenge in using the FBRM to characterize hydrate size. The cumulative distribution in Figure 8 labeled "During Formation" was recorded 2 hours after hydrate nucleation. It is clear from the cumulative distributions that with hydrate formation there is a shift to the left, meaning the average measured chord size decreases. In fact, for all high water cut experiments (oil and water continuous), the average measured chord size decreases on hydrate formation. There is also a simultaneous rise in total measured counts. An increase in counts and a drop in average measured size imply that the FBRM detects a size scale much smaller than the actual agglomerate sizes seen in the PVM.

The FBRM laser most likely measured portions of the rough hydrate surface as individual chords rather than the whole agglomerate. The hydrate agglomerate in Figure 6c is an example of such a rough hydrate surface. Furthermore, the FBRM results may be skewed by the deposition of a hydrate film on the FBRM window and subsequent accumulation. The film repeatedly observed to form on the PVM window most likely formed on the FBRM window as well because both were constructed of identical sapphire material. Measurement of (or through) the film could limit the reliability of the FBRM distribution.

For several experiments, hydrate accumulation increased on the PVM window such that no motion was visible. At the point of this accumulation on the PVM, a drop in counts (sometimes to zero) was observed in the FBRM measurements. Such a correlation suggests that similar accumulations must have formed on the FBRM window, making measurement of the hydrate particle/agglomerate size distribution difficult.

Hydrate Formation from O/W emulsions

Figure 9 is a conceptual picture of hydrate formation and dissociation from O/W emulsions. The beginning emulsion in Figure 9a may be either a simple O/W or a complex w/O/W emulsion. Hydrate forms as shells around the oil drops because, relative to water, oil has a high content of dissolved methane for hydrate formation. Due to shell formation, distinct hydrate particles are present (Figure 9b) in the system; however, there is also extensive agglomeration, facilitated by the high water cut.

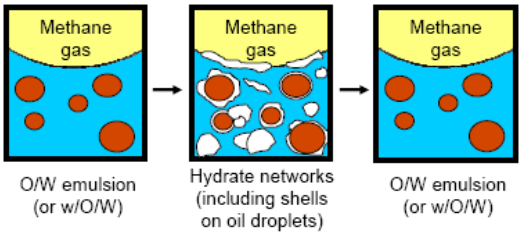

Figure 9. Hydrate formation from an O/W emulsion pressurized with a hydrate forming gas: (a) initial emulsion; (b) after hydrate formation; (c) final emulsion after dissociation of gas hydrate.

The formation of shells on the oil drops effectively traps the oil, making it impossible for the oil to coalesce and become the continuous phase. During heating, the hydrate shells dissociate and the emulsion is of the O/W type (Figure 10c). If the starting emulsion was a w/O/W emulsion (as was the 75 vol% experiment), the multiple emulsion was lost with hydrate formation and dissociation; the w/O/W emulsion returned gradually with continued mixing some time after dissociation completed. The loss of occluded water droplets from the w/O/W emulsion with hydrates to form an O/W emulsion may be due to several factors. For instance, hydrate particles formed from occluded water drops may puncture the oil-external water interface, or if a hydrate shell were to first form between the oil and external water, occluded water drops may move to this solid

interface and wet the hydrate shell and/or also convert to hydrate.

Water continuous emulsions (75 vol%)

Hydrate formation and dissociation from O/W emulsions (including w/O/W emulsions) appeared similar for all water cuts. Formation and dissociation from 75 vol% water is reported here. The PVM images shown in Figure 10 illustrate the changes to the emulsion with hydrate formation and dissociation. The emulsion was originally a w/O/W emulsion (Figure 10a), though not all of the oil drops have occluded water droplets (Figure 10b). Upon hydrate formation, the hydrate formed as shells around the oil droplets (Figure 10c) with agglomerated networks also visible (Figure 10d). With dissociation, essentially no multiple emulsion was visible, only oil droplets in water (Figure 10e), suggesting that hydrate formation broke most of the multiple emulsion. The multiple emulsion returned gradually (2+ hours) with continued mixing (Figure 10f).

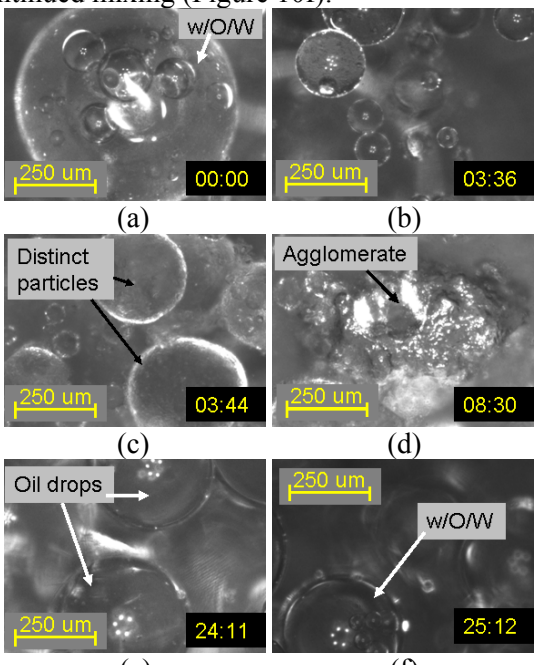

Figure 10. 25 vol% Conroe oil in water: (a) initial w/O/W emulsion; (b) emulsion (some multiple emulsion) 6 min. before nucleation; (c) initial hydrate formation 3 min. after nucleation; (d) large hydrate agglomerate; (e) O/W emulsion 36 min. after the start of dissociation; (f) w/O/W emulsion 97 min. after the start of dissociation.

Conductivity results in Figure 11 again correspond well to the PVM images and elucidate the type of emulsions present. The conductivity plot of Figure 11 has been enlarged to clarify nucleation and dissociation behavior in Figures 12a and 12b. The conductivity was high prior to nucleation (≈7 volts) and increased to 8 volts with nucleation in Figure 12a. Hydrate may have agglomerated and stuck to the electrodes (similar to the W/O experiments), but adhesion would not generate the observed rise in conductivity because the continuous phase is already water. Instead, the conductivity rises at nucleation most likely because hydrate forms at the oil-water interface, trapping oil behind hydrate shells. Because the oil is entirely trapped inside hydrate shells, the conductivity represents essentially pure water. The system is a slurry of hydrate particles and agglomerates (with trapped oil) in water.

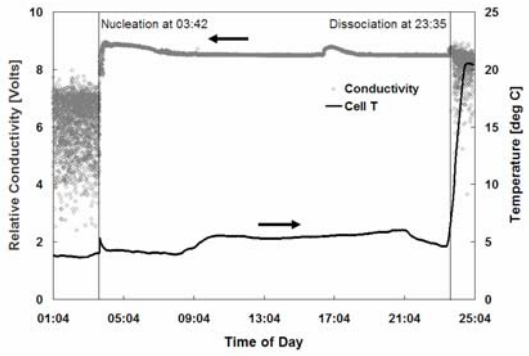

Figure 11. Conductivity and temperature measurements for hydrate formation and dissociation from 25 vol% Conroe oil in water.

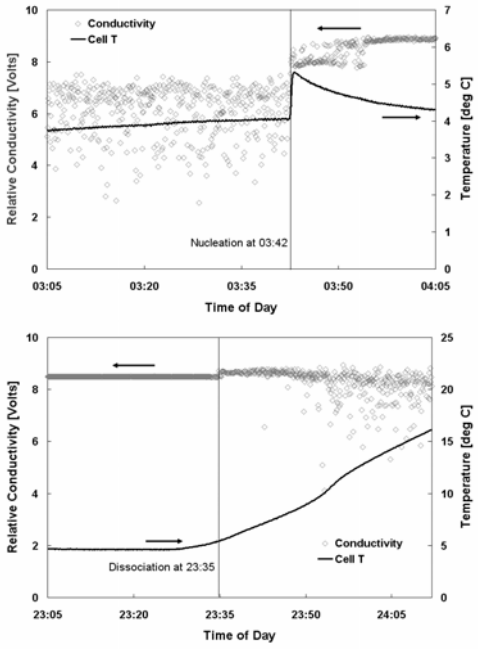

Figure 12. Conductivity and temperature measurements of nucleation (a) and dissociation (b) for 25 vol% Conroe oil in water.

With the start of dissociation (Figure 12b), the conductivity remained high until the shells dissociated enough to release the trapped oil, leaving an O/W emulsion. The conductivity fluctuated some with the return of the emulsion (a simple O/W). The scatter in the data increased with continued mixing as the multiple w/O/W emulsion slowly returned (See Figure 10f). Bridging of the electrodes by the passing of large oil droplets swollen with occluded water may cause the conductivity fluctuations, with the oil droplets having a lower conductivity than the water continuous phase. Furthermore, as water occlusion increases, the effective water cut decreases, leading to a gradual decrease in conductivity from that of a simple O/W system.

The FBRM results (See Figure 13) validate the loss of the multiple emulsion with hydrate formation and dissociation. If the multiple emulsion were to break, occluded water droplets would coalesce with the continuous phase, and the oil drops would subsequently shrink from their swollen state. The average droplet size (and average measured chord length) would then decrease due to the absence of large swollen oil drops. Consequently, the FBRM CLD following dissociation and heating shifted to the left relative to the pre-nucleation distribution, having a significant loss in large size counts compared to the pre-nucleation emulsion. In fact, the mean chord length drops between these two distributions from 35 to 23 μm, and the square weighted mean decreases from 254 to 112 μm. The square weighted mean is reported because it emphasizes changes in the larger size range, demonstrating the significant decrease in large oil droplets due to multiple emulsion destabilization.

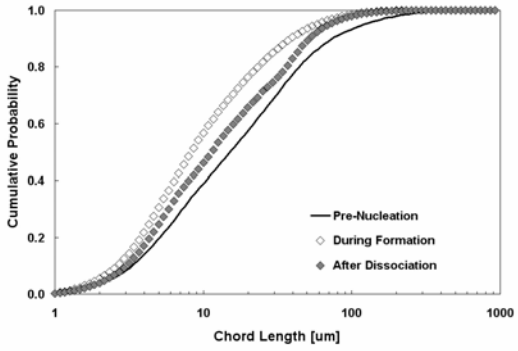

Figure 13. FBRM CLDs for 25 vol% Conroe oil in water. Distributions are the average of 10 FBRM measurements. Pre-nucleation results are from 15 min. prior to nucleation (at 4°C), during formation results are taken at the peak in measured counts 3 hrs. after nucleation, and after dissociation is taken 2 hrs. after the start of dissociation (at 20°C).

In Figure 13 the distribution during formation is again shown to demonstrate the unreliability of the FBRM measurements of particle size during hydrate formation. An overall decrease in average chord length is measured with formation despite the extensive agglomeration in the system (seen using the PVM).

DISCUSSION OF RESULTS

The observed effects of hydrate formation and dissociation on the water-Conroe crude oil emulsions can be summarized by two key conclusions.

1. Hydrate formation at the interface prevents an overall change to the emulsion continuous phase until dissociation begins.
2. With dissociation, remaining hydrate networks appear to promote O/W emulsification.

Hydrate formation at the interface

Hydrate nucleation from either an oil or a water continuous emulsion occurs at the interface between droplets and the continuous phase. Hydrate shells form around water or oil drops in a W/O or O/W emulsion, respectively. PVM images show distinct spherical particles in both emulsion types representing this shell formation. Shell formation effectively traps the emulsified liquid phase such that an inversion cannot occur until dissociation breaks up the shells, freeing the emulsified liquid phase. In these high water content systems, excess water facilitates rapid agglomeration – either from agglomeration between wet hydrate particles (W/O and O/W emulsions) or from formation at the gas-water interface (O/W emulsion). Hence, PVM images also show extensive agglomeration.

It was originally thought before performing this work that as hydrate would form from an O/W emulsion close to the inversion, the emulsion would catastrophically invert to W/O. When hydrate is formed, water is converted to solid hydrate, which causes the overall volume of external liquid phase water to decrease. If it were to decrease sufficiently, the emulsion might catastrophically invert, but this did not occur.

After 8 hours of formation, approximately 8-12% of the water converted to hydrate, depending on the O/W experiment. Additionally, some unconverted water was most likely occluded in the hydrate networks during formation and agglomeration. The combined decrease to the effective liquid water phase volume (from conversion to solid hydrate and occluded water) would be enough to decrease the water cut for the 71 vol% water experiment (not reported here), and perhaps the 75 vol% experiment, past the catastrophic inversion line (predicted somewhere between 68-71 vol%). Though the effective volume of water decreased, no inversion was observed because the oil was trapped inside hydrate shells, making it impossible for the oil to emulsify the water and become the external phase.

Dissociation and O/W emulsification

It can be concluded from the three experiments discussed that the hydrate event (formation and dissociation) changes the emulsion formulation in favor of O/W emulsification. The W/O emulsion far from inversion (60 vol% water) ended as an o/W/O emulsion (occluded oil droplets in water drops obey the decrease in formulation), the W/O emulsion near inversion (68 vol% water) inverted to an O/W emulsion, and the w/O/W emulsion (75 vol%) ended dissociation as an O/W emulsion, though the latter two did ultimately become w/O/W emulsions. Each of the three emulsions changed at some point during dissociation in favor of oil in water emulsification (representing a decrease in the overall formulation).

One possible explanation for the change in emulsion type is that partial dissociation introduces smaller hydrate flakes or networks (like those observed in the PVM images gathering at the water-oil interface) into the system. These flakes may have acted like hydrophilic solids, promoting O/W rather than W/O emulsification, the same way hydrophilic particles promote O/W emulsification, even causing an inversion from W/O to O/W [10,23]. Without these solids, the natural surfactants in the crude oil would control the emulsion type, favoring W/O, except at extreme water cuts where the volume controls. Such hydrate flakes would match the water-wet hydrates observed by Hoiland et al. [8,9].

Assuming that hydrophilic hydrate flakes change the water chemistry such that water can emulsify the crude oil, two possible mechanisms explain the change in emulsion type with dissociation for the W/O emulsions:

1. Crude oil is gradually occluded in the water drops (forming an o/W/O emulsion). The water drops swell and may perhaps reach a critical packing fraction, causing the emulsion to invert from oil to water continuous [13,24].
2. Water, with hydrate flakes present, is released following sufficient dissociation of the shells. Re-emulsification is performed at a decreased formulation compared with the original emulsion, resulting in new emulsified states (either o/W/O or O/W).

The first mechanism was observed for the 60 vol% experiment; PVM images showed gradual occlusion of oil droplets in water drops forming an o/W/O emulsion coexistent with hydrate flakes. However, conductivity measurements and PVM images do not confirm that gradual occlusion of oil droplets in water drops led to a critical packing and a catastrophic inversion for the 68 vol% experiment.

In fact, the observed inversion results for 68 vol% better support the second proposed mechanism. First, hydrate dissociation destabilizes the W/O emulsion. This same destabilization due to formation and dissociation of hydrate agglomerates has been observed by authors who have used differential scanning calorimetry (DSC) [3,7]. At some point following the start of dissociation of agglomerates, sufficient hydrate will dissociate to release the occluded phase (water for the W/O case). According to this second proposed mechanism, once trapped liquid water has been released for the W/O emulsion cases, continuous mixing, used here but not in the DSC studies, enables the formation of a different emulsion. Hydrate flakes in the water phase make it possible for the released water to emulsify the oil.

When the oil and water are re-emulsified, a different emulsion forms because the formulation has decreased (due to the remaining hydrate in the water phase). The new emulsion is either an o/W/O emulsion, or in the case of inversion, O/W. This inversion is not the typical transitional type because the formulation is not decreased gradually from favoring W/O to O/W. Rather, the initial emulsion prior to hydrate formation had one

formulation, favoring W/O, and the mixture is re-emulsified at a second formulation, favoring O/W, after the start of hydrate dissociation.

A combination of the two mechanisms may best explain the behavior for oil continuous emulsions. The emulsion is destabilized by the hydrate event. For water cuts not near the inversion (60 vol%), the emulsion will remain oil continuous; however, the dissociating hydrate in the water phase makes it possible for the water drops to emulsify oil droplets from the continuous phase. When the emulsion is near the inversion (68 vol%), re-emulsification at the new formulation alone causes an inversion – gradual occlusion is not necessary.

Hydrophilic hydrate flakes change the water continuous emulsions as well, adding increased stability to the O/W emulsion. In the 75 vol% w/O/W case, the multiple emulsion breaks with hydrate formation, leading to a hydrate-O/W mixture. The decreased formulation with dissociation (combined with the high water content) further promotes the formation of an O/W emulsion with dissociation.

Ultimately, the O/W emulsions formed from the 68 and 75 vol% emulsions underwent gradual occlusion to form w/O/W emulsions. With the continued dissociation of hydrate flakes, it may not be possible for the water phase to entirely stabilize the oil drops and prevent occlusion and w/O/W formation.

CONCLUSIONS

This work is directly applicable to high water cut production scenarios. While the flow conditions in a pipeline may lead to stratified layers of emulsions and even free water, the understanding of how hydrate forms and dissociates from various high water cut emulsions is essential. At high water cuts, the system can rapidly agglomerate with hydrate formation, while dissociation can lead to a significant change in the emulsion type. Inhibition can be costly at high water cuts, but it must be considered due to the risk of immediate agglomeration and plug formation with hydrates.

For both W/O and O/W emulsions, hydrate was observed to form both distinct particles and large agglomerates, facilitated by the high water cut. Distinct particles represent shell formation on water and oil drops for the W/O and O/W emulsions, respectively.

It has been shown for the water-Conroe crude oil system that hydrate formation from a W/O emulsion leads to rapid agglomeration in the system. Dissociation of these large agglomerates can lead to large water droplets and perhaps even a free water phase. Re-emulsification can significantly alter the emulsion type, forming either an o/W/O emulsion or inverting to an O/W or w/O/W emulsion as hydrate appears to change the formulation in favor of O/W emulsification.

Conversely, no inversion was observed for the water continuous cases, and the hydrate event added further stability to the O/W emulsion. Hydrate formation and dissociation from a w/O/W emulsion broke the multiple emulsion, forming an O/W emulsion. The multiple emulsion returned following extended mixing. It is proposed that an O/W emulsion does not invert with the hydrate event because (1) during hydrate formation the hydrate traps the oil within hydrate shells, making coalescence impossible and (2) during dissociation the hydrate decreases the formulation, increasing the tendency for water to emulsify oil.

ACKNOWLEDGEMENTS

The authors would like to thank the Center for Hydrate Research Consortium members for support of this work as well as Dr. Johan Sjoblom, Dr. Jean-Louis Salager, and Dr. Steve Dec for assistance with portions of this work.

REFERENCES

[1] Sloan ED. *Hydrate Engineering*. Richardson, TX: Society of Petroleum Engineers Inc., 2000.

[2] Sloan ED, Koh CA. *Clathrate Hydrates of Natural Gas (3rd Edition)*. Boca Raton, FL: CRC Press – Taylor and Francis Group, 2008.

[3] Lachance J. *Investigations of gas hydrates using differential scanning calorimetry with water-in-oil emulsions*. Golden, CO: M.S. thesis, Colorado School of Mines, 2008.

[4] Palermo T, Mussumeci A, Leporcher E. *Could hydrate plugging be avoided because of surfactant properties of the crude and appropriate flow conditions?* Offshore Technology Conference 2004;OTC 16681.

[5] Sinquin A, Palermo T, Peysson Y. *Rheological and flow properties of gas hydrate suspensions*. Oil and Gas Science Technology - Rev. IFP 2004;59:41-57.
[6] Turner D. *Clathrate hydrate formation in water-in-oil dispersions*. Golden, CO: Ph.D. thesis, Colorado School of Mines, 2005.
[7] Palermo T, Arla D, Borregales M, Dalmazzone C, Rousseau L. *Study of the agglomeration between hydrate particles in oil using differential scanning calorimetry (DSC). In: Proceedings of 5th International Conference on Gas Hydrates, Trondheim, Norway, 2005*.
[8] Hoiland S, Askvik KM, Fotland P, Alagic E, Barth T, Fadnes F. *Wettability of Freon hydrates in crude oil/brine emulsions*. Journal of Colloid and Interface Science 2005;287:217-225.
[9] Hoiland S, Borgund AE, Barth T, Fotland P, Askvik KM, 2005. *Wettability of Freon hydrates in crude oil/brine emulsions: the effects of chemical additives. In: Proceedings of 5th International Conference on Gas Hydrates, Trondheim, Norway, 2005*.
[10] Binks BP. *Particles as surfactants – similarities and differences*. Current Opinion in Colloid and Interface Science 2002;7:21-41.
[11] Salager JL, Marquez L, Pena A, Rondon M, Silva F, Tyrode E. *Current phenomenological know-how and modeling of emulsion inversion*. Industrial & Engineering Chemistry Research 2000;39:2665-2676.
[12] Salager JL. *Emulsion phase inversion phenomena*. In: Sjoblom J, editor. Emulsions and Emulsion Stability (2nd Edition). Boca Raton, FL: CRC Press – Taylor & Francis, 2006. p. 185-226.
[13] Zambrano N, Tyrode E, Mira I, Marquez L, Rodriguez MP, Salager JL. *Emulsion catastrophic inversion from abnormal to normal morphology. 1. Effect of the water-to-oil ratio rate of change on the dynamic inversion frontier*. Industrial & Engineering Chemistry Research 2003;42:50-56.
[14] Becher P. *Emulsions: Theory and Practice (3rd Edition)*. New York: Oxford University Press, 2001.
[15] Schramm LL. *Emulsions, Foams, and Suspensions*. Germany: Wiley-VCH, 2005.
[16] Mettler-Toledo Lasentec® Product Group. *Lasentec® D600 Hardware Manual*. Richmond, WA: Mettler-Toledo AutoChem, Inc., 2001.
[17] Mettler-Toledo Lasentec® Product Group, *Lasentec® PVM User Manual*. Richmond, WA: Mettler-Toledo AutoChem, Inc., 2002.
[18] Dec SF, Gill SJ. *Steady-state gas dissolution flow microcalorimeter for determination of heats of solution of slightly soluble gases in water*. Review of Scientific Instruments 1984;55:765-772.
[19] Greaves D. *The effects of hydrate formation and dissociation on high water content emulsions*. Golden, CO: M.S. thesis, Colorado School of Mines, 2007.
[20] Kokal S. *Crude oil emulsions: a state-of-the-art review*. SPE Production and Facilities 2005;20:5-13.
[21] Austvik T, Li X, Gjertsen LH. *Hydrate plug properties: formation and removal of plugs*. Gas Hydrates: Challenges for the Future Annals of the New York Academy of Science 2000;912:294-303.
[22] Taylor CJ. *Adhesion force between hydrate particles and macroscopic investigation of hydrate film growth at the hydrocarbon/water interface*, Golden, CO: M.S. thesis, Colorado School of Mines, 2006.
[23] Hannisdal A, Ese MH, Hemmingsen PV, Sjoblom J. *Particle-stabilized emulsions: effect of heavy crude oil components pre-adsorbed onto stabilizing solids*. Colloids and Surfaces A 2006;276:45-58.
[24] Sajjadi S, Zerfa M, Brooks BW. *Dynamic behaviour of drops in oil/water/oil dispersions*. Chemical Engineering Science 2002;57:663-675.